Carbohydrate Polymers 297 (2022) 120030

Contents lists available at ScienceDirect

Carbohydrate Polymers

journal homepage: www.elsevier.com/locate/carbpol

Preparation and characterization of some cellulose derivatives nanocomposite films

Fatma Özge Gökmen [a,b,*], Nursel Pekel Bayramgil [a]

[a] Hacettepe University, Faculty of Science, Chemistry Department, 06800 Ankara, Turkey
[b] Bilecik Şeyh Edebali University, Central Research Laboratory, 11230 Bilecik, Turkey

ARTICLE INFO

Keywords:
Cellulose
Hydroxyethyl cellulose
Hydroxypropyl methylcellulose
Hydroxypropyl cellulose
Nano SiO_2

ABSTRACT

One of the most studied biocomponents is cellulose and its derivatives. Chemical structures of the nanocomposite films were investigated by Fourier Transform Infrared Spectroscopy (FT-IR) and X-Ray Diffraction (XRD) analyses. In the Scanning Electron Microscope (SEM) images taken at 5000 x magnification, the films with the best dispersion of nano-reinforcements; are amine modified nano SiO_2 doped 2-hydroxyethyl cellulose (2-HEC) and hydroxypropyl cellulose (HPC) films. SiO_2 dispersion has not been homogeneous in neutral nano SiO_2 doped HPC and hydroxypropyl methylcellulose (HPMC) films. On the other hand, in the amine modified nano SiO_2 doped HPMC film, micron-size agglomerations were observed on the film surface. When the thermal resistance of the films was examined, it was determined that the amine modified nano SiO_2 doped HPMC film was the highest at 344 °C. When stress-strain values were compared, amine modified nano SiO_2 doped HPMC film was the best film sample with a strain value of 101.7 %.

1. Introduction

Cellulose is a renewable, environmentally friendly, low-cost, thermal, and chemically stable polymer that is abundant in nature (Chen et al., 2018; Hu et al., 2020; Wang et al., 2016). It is also biodegradable material. It is known that in the future, celluloses will partially replace synthetic polymers synthesized as petroleum derivatives. The possibility of using celluloses in this way is promising (Jedvert & Heinze, 2017; Li et al., 2017; Tu et al., 2020; Yuan et al., 2015). Celluloses are common in the cell walls of plants and marine organisms. Cellulose is also synthesized by algae, bacteria, and fungi through microbial biosynthesis (Liu et al., 2020). There are hydroxyl groups on the carbon atoms that can form hydrogen bonds between the cellulose molecules. These groups play a very important role in controlling and improving the physicochemical properties of cellulose (Moon et al., 2011; Wang et al., 2020). Cellulose is a natural polymer and the length of the polymer chain depends on the cellulose source. Cellulose is not found in nature as a molecule, but as a fiber formed by molecular chains. Cellulose has high mechanical strength, chemical resistance, good thermal stability, biocompatibility, and excellent physicochemical properties (Du et al., 2018; Du et al., 2020; Kargarzadeh et al., 2018). On the other hand, cellulose has disadvantages such as poor thermoplastic properties and easy molding. The molecular structure of cellulose is not suitable for easy processing. Due to the strong hydrogen bonds of cellulose, its plain form is insoluble in water. This situation is an obstacle to overcome in practice (Bao et al., 2021; Sayyed et al., 2019; Yamane et al., 2015) and the cellulose must be modified (Arca et al., 2018). These modifications can be physical, chemical, or biological (Cao & Tan, 2002; Gabriel et al., 2014; Menon et al., 2017). These modified cellulose structures are defined as cellulose derivatives. Cellulose derivatives, which are a group of natural polymers, have film-forming ability, cross-linking, hydrogel, cryogel, and aerogel-forming properties. Cellulose chains are interconnected by intramolecular and intermolecular hydrogen bonds and Van der Waals forces. The exceptional rheological properties of cellulose derivatives make these materials remarkable (Esmaeilirad et al., 2016; Roshan & Asef, 2010; Udayakantha et al., 2019; Yang et al., 2015). Cellulose derivatives, which are easily soluble in water, are used in many application areas from food to cosmetics, from pharmaceuticals to textiles (Badulescu et al., 2008; Liu et al., 2021; Petit & Wirquin, 2013; Spirk, 2018). Cellulose derivatives such as hydroxyethyl methyl cellulose (HEMC) and hydroxypropyl methylcellulose (HPMC) originate from biomass which has a mesoporous morphological structure (Hoang & Dat, 2021). Carboxymethyl cellulose (CMC), hydroxyethyl cellulose (HEC), carboxymethyl hydroxyethyl cellulose (CMHEC) are water-

* Corresponding author.
E-mail addresses: fatmaozge.gokmen@bilecik.edu.tr (F.Ö. Gökmen), nursel@hacettepe.edu.tr (N. Pekel Bayramgil).

https://doi.org/10.1016/j.carbpol.2022.120030
Received 29 June 2022; Received in revised form 21 August 2022; Accepted 22 August 2022
Available online 27 August 2022
0144-8617/© 2022 Elsevier Ltd. All rights reserved.

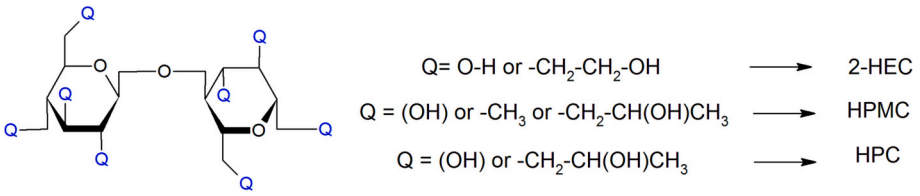

Fig. 1. Chemical structure of cellulose derivatives.

soluble cellulose derivatives (Arca et al., 2018; Marinho, 2013). Three different cellulose derivatives were used in this study. Each cellulose was preferred due to its different physicochemical properties. The effect of SiO_2 nanoparticles dispersed on hydroxypropyl methylcellulose (HPMC), hydroxypropyl cellulose (HPC), and 2-hydroxyethyl cellulose (2-HEC) with different physicochemical properties on films is discussed. The reason why HPMC is preferred; it can be developed to increase the bioavailability of active pharmaceutical ingredients by adjusting its solubility in water (Borlinghaus et al., 2022). The fact that it is inexpensive and easy to find also provides an additive advantage. HPMC has been used as a support material for metal catalysts in previous studies. Based on this, HPMC has assumed the role of support material similar to nano SiO_2 reinforcement materials for this study. It is non-toxic and biologically compatible (Kesevan et al., 2022). It has excellent film-forming ability (Kesevan et al., 2022; Luo et al., 2020) and excellent mechanical properties (Wang et al., 2022). HPC is one of the important cellulose derivatives, which is water soluble, biodegradable, and non-toxic just like HPMC. It is widely used in the production of smart materials, biomedicine, pharmacology, and cosmetics (Bulut & Turhan, 2021). HPC is a temperature-sensitive cellulose derivative. It is interesting to develop the properties of heat-sensitive material that can be used in controlled release applications by taking advantage of this feature (Bulut & Turhan, 2021). Low viscosity is a disadvantage that must be overcome. It is a cellulose derivative approved by the FDA (U.S. Food and Drug Administration) (Saraiva et al., 2021). Finally, 2-HEC was used as a cellulose derivative in this study. The most important reason for the preference is that it can be formed easily and is biocompatible (Mutalik et al., 2006). All three cellulose derivatives are environmentally friendly and, despite being a non-ionic polymer group, additional interaction difficulties are not experienced in composites obtained with nanomaterial reinforcements. Polymers are classified into two groups, synthetic and natural. Natural polymers are called “biopolymers” because of their biodegradable properties. Biopolymers can be obtained by 3 different methods; (i) chemically, (ii) as an extraction product, and (iii) biologically (Gopi et al., 2019). Natural polymers are the most promising group of biomaterials (Kulshrestha & Mahapatro, 2008). Natural polymers do not have good strength properties, nor are they resistant to temperature (Ramakrishna et al., 2001). These weaknesses of natural polymers can be eliminated by developing them as composite materials formed with two or more components. Thus, different properties of each component that make up the composite appear in a new material than when they were alone (Josmin & Kuruvilla, 2012). Biocomposites consist of reinforcement or filler materials consisting of a polymer matrix and various particles that affect the mechanical and physicochemical properties of this matrix. If these particles are in nano size, the new material is called “nano biocomposite”. “Green polymers” from sustainable sources offer a biodegradable, environmentally friendly alternative to synthetic polymers (Song et al., 2018). Titanium dioxide (TiO_2) and silicon dioxide (SiO_2) are the most remarkable reinforcement nanoparticles that provide low toxicity, improved scratch resistance, stickiness, transparency, and high stability at different pHs (Cristea et al., 2010; Fufa et al., 2013; Pacheco et al., 2021; Sow et al., 2011). Nano SiO_2 is a frequently preferred reinforcement material due to its high surface area and adjustable porosity properties for different application areas. By modifying the surface of Nano SiO_2, its functionality can be extended in many areas (Bettini et al., 2015; Regan et al., 2019). The most common usage area is adsorbent and super adsorbent materials in adsorption systems (Bettini et al., 2022). Green nanomaterial technologies are of great importance today (Lu & Ozcan, 2015). Studies carried out with these two approaches are the focus of attention on a global scale (Nasir et al., 2017). It is important to improve bionanocomposites that are biologically compatible with the human body and are not harmful to the environment for different usages. In this study, bionanocomposite films were obtained by adding two types of nano SiO_2 (neutral and amine-modified) as reinforcement to 2-HEC, HPMC, and HPC solutions separately and their main properties were compared with each other. Like amine modified nano SiO_2, amine modified adsorbents noticeably increase the adsorption uptake of various toxic molecules and improve the reuse of materials, which indicates their high stability. It is important to note that the negative surface charge can be used advantageously for subsequent surface modifications using silane chemistry, via covalent bonding, or through physical adsorption or electrostatic interactions. Nanocomposites that are prepared with three different silica doping of cellulose derivatives are the strongest hypothesis for this study, by using silica nanoparticles in the cellulose structure in preferred application areas stands out as a silica-based cellulose structure. Silica nanoparticles can be modified or mineral materials with high silica content can be used. Herein, biopolymers (cellulose derivatives) as green chemicals and nano SiO_2, which are both different and widely used as both green chemistry and nano reinforcement materials, were studied. Two different commercially synthetic SiO_2 were used as additives. One of them was provided as amine modified hydrophilic (*hf* nano SiO_2) and the other as unmodified (nano SiO_2). It has ensured that the nano-sized SiO_2 can be easily dispersed in cellulose films. Recent studies mostly focus on cellulose derivatives which are doped by except inorganic particles, for example, chitosan, snail mucus, starch, etc. (Antosik et al., 2019; Filippo et al., 2021; Zhang et al., 2020). The biggest novelty presented in this study is that SiO_2 nanoparticles are used as a particle in the cellulose derivatives composites and determined the physicochemical properties. Afterward, amorphous volcanic glass minerals were selected and used with the cellulose derivatives to elicit the differences and similarities between nano SiO_2 particles and nano-sized expanded perlite. Obtained nanocomposites will be role models in many application areas from human skin compatibility to new generation food packaging packages in future studies.

2. Experimental

The cellulose derivative nanocomposite films were produced in the presence of a crosslinking agent. Silica nanoparticles and expanded perlite were selected as reinforcement materials.

3. Materials and methods

Materials used throughout this study; amine modified hydrophilic *(hf)* nano SiO_2 (10–20 nm, 99.8 %, Skys NanoMaterials), nano SiO_2 (15–20 nm, 99.5 %, Skys NanoMaterials) (Sigma-Aldrich), *N*-methylenebisacrylamide (N, N-MBAAm) (Sigma-Aldrich), ceric ammonium nitrate ($Ce(NH_4)_2(NO_3)_6$) (Sigma-Aldrich), 2-hydroxyethyl cellulose (2-HEC), hydroxypropyl cellulose (HPC), and hydroxypropyl methylcellulose (HPMC) were supplied by Sigma-Aldrich.

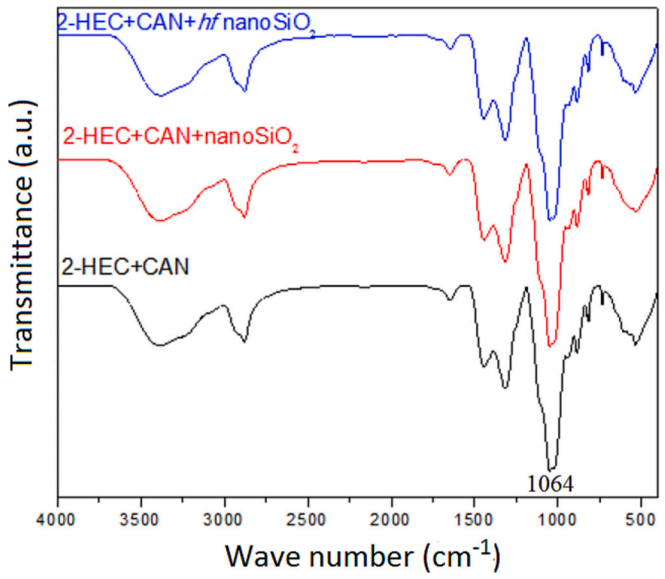

Fig. 2. FT-IR spectrum of cross-linked 2-HEC, 2-HEC-nano SiO_2 and 2-HEC -*(hf)* nano SiO_2.

3.1. Preparation of cellulosic nanocomposite films

The cellulose-derived nanocomposite films were prepared by the solution casting method and named "cellulosic nanocomposite films". The mixture was poured into 60 × 15 mm glass petri dishes in equal volumes (20 mL). The solutions were left to dry for one week under room conditions. Then, the nanocomposite cellulose derivatives films were separated from the glass petri dishes with the help of a micro spatula and forceps without being damaged. Nano-reinforcement materials were initially added to each cellulose solution as a mixture. 5%wt. aqueous solutions were prepared from 2-HEC, HPC, and HPMC, separately. 0.08 g of ceric ammonium nitrate (CAN) was added to each solution. The solutions were mixed in an ultrasonic bath at 60 °C. In addition, films without CAN were also prepared by the same method for comparison. Amine-modified nano SiO_2 and neutral nano SiO_2 were used as reinforcements. After determining the amount of 0.0010 g nano SiO_2 with the best particle distribution, the studies were carried out with this amount of SiO_2 supplementation. The chemical structure of the

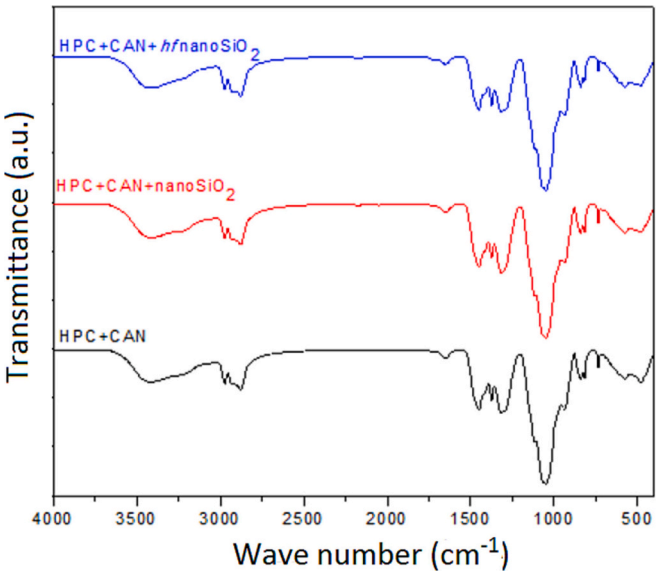

Fig. 4. FT-IR spectrum of cross-linked HPC, HPC-nano SiO_2 and HPC–*/(hf)* nano SiO_2.

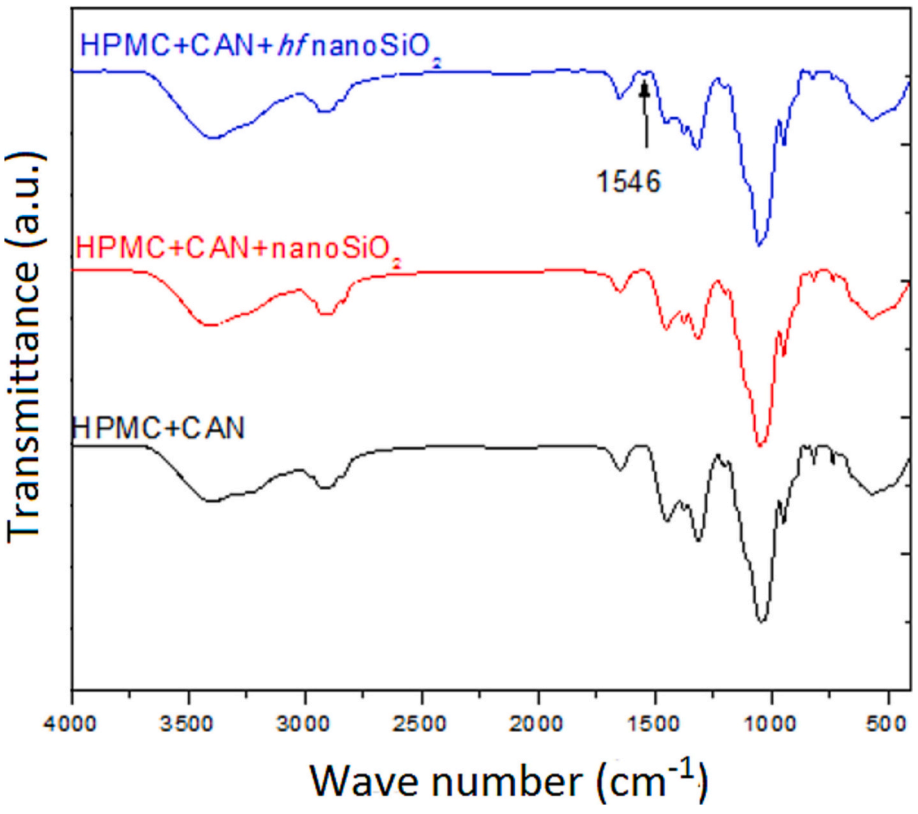

Fig. 3. FT-IR spectrum of cross-linked HPMC, HPMC-nano SiO_2 and HPMC- *(hf)* nano SiO_2.

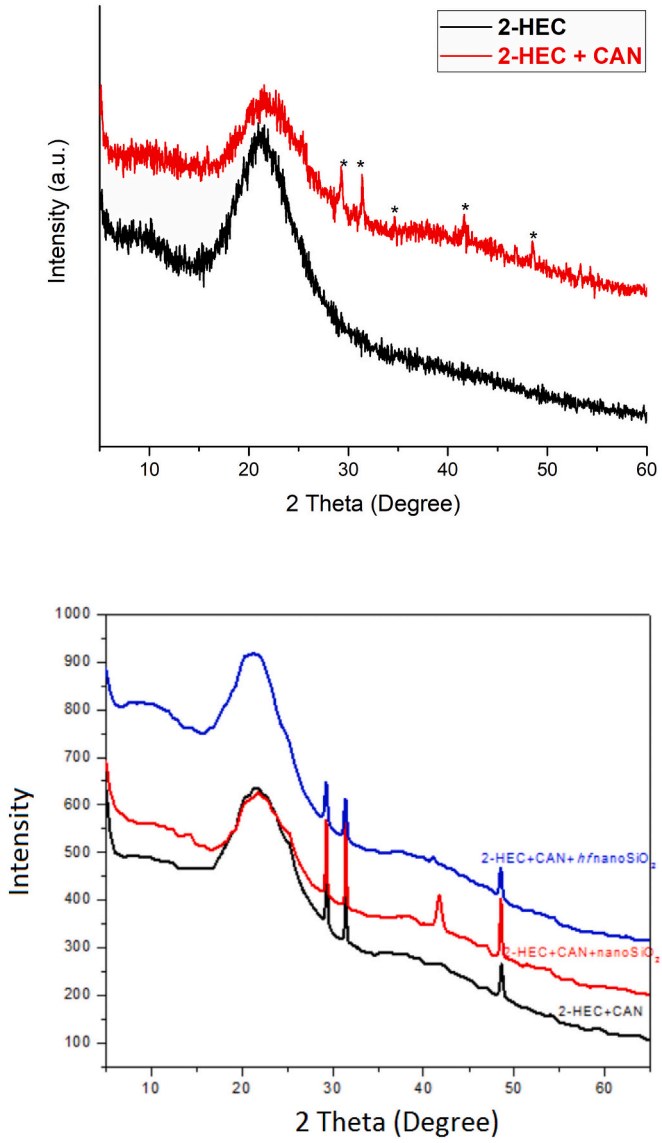

Fig. 5. XRD spectra of cross-linked and non-cross-linked 2-HEC films.

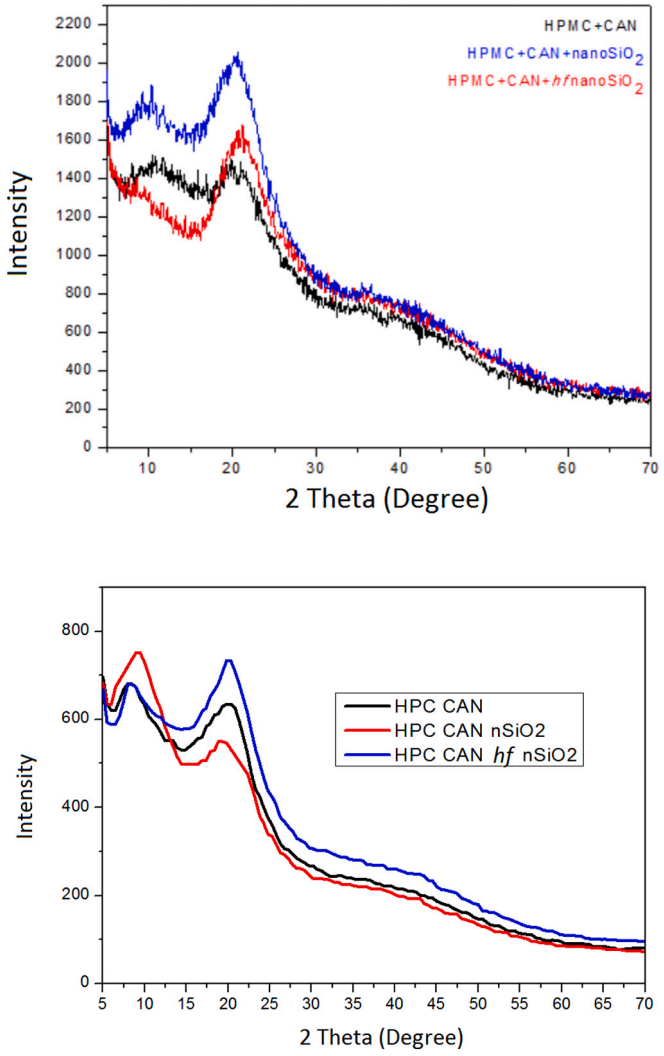

Fig. 6. XRD pattern of cross-linked HPMC, HPMC- nano SiO_2, HPMC- *(hf)* nano SiO_2.

celluloses used in this study is shown in Fig. 1.

3.2. Characterization of cellulose deviations-based nanocomposite films

Functional groups of the components were determined by FT-IR spectroscopy using the ATR technique by Perkin Elmer, Spectrum 100 with a resolution of 4 cm^{-1}, within the range 400–4000 cm^{-1}. Structural properties of the nanocomposite films were investigated by X-Ray diffraction (XRD) measurements, using a Panalytical Empyrean diffractometer with Cu*K*a radiation of 45 kV, 40 mA, and scanning range between 5° and 65°. Morphological properties of the films were obtained by Field Emission Scanning Electron Microscopy (FESEM), Carl Zeiss, Supra 40VP microscope, with the samples sputter-coated previously under vacuum with platinum, and applied 10 kV of acceleration voltage. TGA analyzes were performed with a SETERAM brand, simultaneous TG/DTA device. Heating was carried out in a temperature range of 25 °C–750 °C, at a heating rate of 10 °C·min^{-1} and in an N_2 atmosphere.

3.3. Universal mechanical test

Stress-strain tests were performed at room temperature with a Baehr (Germany) Universal testing machine with a maximum load of 10 kN. The starting distance between the jaws was kept at 40 mm. Three different samples were cut from each cellulose film and thickness measurements were made from three different places of each sample with a digital micrometer. For the stress-strain calculation, the average values obtained from the tested samples were considered. The samples were cut with a cutting apparatus under ASTM 638 standard Type V.

Stress-strain results were obtained with the calculation method under EN ISO 527-1 standard. All tensile values (σ) in MPa are based on the initial cross-sectional area of the test specimens. The stress values of the films were calculated by Eq. (1).

$$\sigma = F, \text{Force (Newton)}/A, \text{Area } (\text{mm}^2) \quad (1)$$

Strain values (ε) are in % based on the jaw separation distance calculated by Eq. (2).

$$\varepsilon\ (\%) = 100^*(\Delta L/L_0) \quad (2)$$

Here, L_0 is the initial measurement distance of the test specimen in mm between the jaws, and ΔL is the initial elongation distance of the test specimen between the jaws.

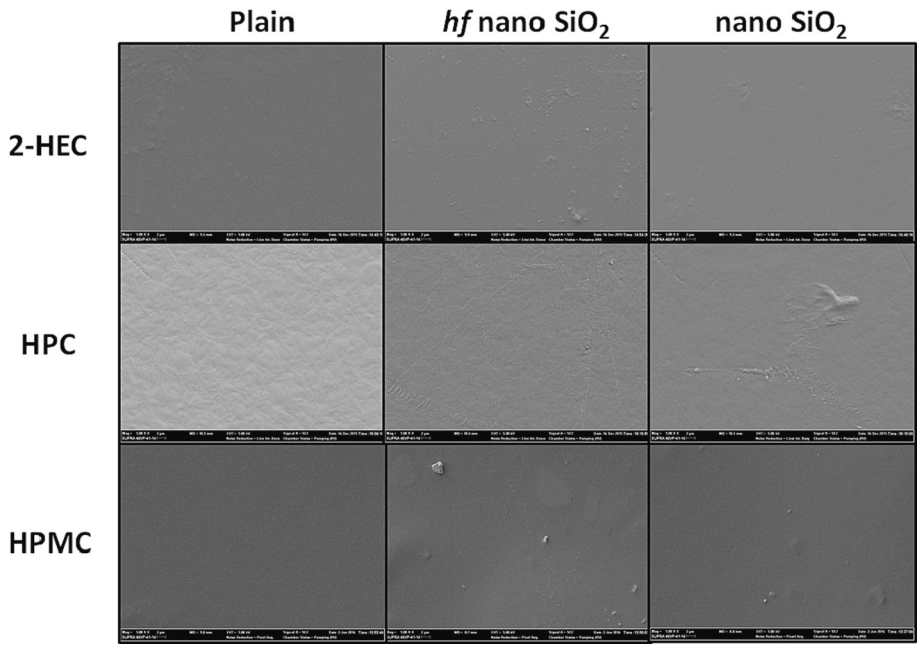

Fig. 7. SEM images of plain/doped 2-HEC, HPC and HPMC films.

4. Results and discussion

4.1. FT-IR analysis

FT-IR spectra of cross-linked 2-HEC film, amine-modified nano SiO_2, and neutral nano SiO_2 doped 2-HEC nanocomposite films were given in Fig. 2. In the spectrum, the band observed at 1064 cm^{-1} belongs to the -C-O-C- glycoside group of cellulose while the band at 3420 cm^{-1} shows OH groups arising from water molecules. In the literature, the -C-O-C- glycosides have been given at 1150–1040 cm^{-1} (Taghizadeh & Seifi-Aghjekohal, 2015). Bands at 1640 cm^{-1} and 1350 cm^{-1} show C-OH bending, and stretching vibrations, respectively. 2945 cm^{-1} gives the aliphatic stretching vibration, and 2940 cm^{-1} gives the CH_2 stretching vibration of cellulose rings. Due to the small amount of nano SiO_2 as reinforcing material used, 2-HEC films did not show an additional functional group. The interactions that occur through glycoside bonds in the cellulose structure can be defined as weak H-bond interactions (Wohlert et al., 2022). Absorption bands at 1086, 795, and 460 cm^{-1} can be assigned to the valence asymmetric, symmetric, and deformation vibration of Si–O–Si bonds, respectively (Angelova et al., 2012; Rangelova et al., 2018). Also, the band at 1203 cm^{-1} originates from the shoulder Si–O–Si junction (Angelova et al., 2019). However, due to the low amount of SiO_2, the intensities of the peaks could not be seen because they were below the other bands.

The FT-IR spectra of plain and nano SiO_2 reinforced HPMC films are given in Fig. 3. The glucose ring of the HPMC was seen at 1050 cm^{-1}. Two shoulder-shaped bands between 1090 and 1130 cm^{-1} have been seen in other studies (Akinosho et al., 2013) and have shifted to 1300–1450 cm^{-1} in Fig. 3. The first of these shoulders represents the secondary alcohol group in the structure, and the second represents the OH band belonging to the primary alcohol group. The 2850 cm^{-1} peak indicates the C—H stretching vibrations of the methyl group. According to Fig. 3, it is seen that a peak at 1546 cm^{-1} occurs in the composite where the HPMC film is doped with amine-modified nano SiO_2. This peak resulted from the hydrogen bonding of the nitrogen (-NH) in the structure with the hydrogen of the OH groups in HPMC.

FT-IR spectra of nano SiO_2 doped and plain HPC films are given in Fig. 4. According to the literature, in addition to the broad peak –OH bonds appearing in the 3500 cm^{-1} region, the reason may have been observed due to the effects from SiO_2, although it was doped in a very small amount due to the cellulose structure (Angelova et al., 2012). Here, the increasing intensity of the peak indicates that the amine-modified nano SiO_2 and nano SiO_2 were bounded to the cellulose structure.

4.2. XRD analysis

In XRD spectra (Fig. 5) taken to show the crosslinking effect separately, the amorphous nature of cellulose for crosslinked 2-HEC and non-crosslinked 2-HEC slightly decreased after the addition of crystalline CAN. The crystalline peaks in the XRD spectra belong to the crosslinking agent CAN. These peaks not only demonstrate the size reduction of the particles but also highlights the amorphous nature of cellulose derivatives by proving the findings of thermal analysis. 2-HEC, HPC, and HPMC matrix samples have a higher effect on amorphization than CAN spectrum (Fathi et al., 2022). In the observed XRD spectra of the plain 2-HEC film and nano SiO_2-doped 2-HEC films in Fig. 5 (continued) (XRD pattern of cross-linked 2-HEC, 2-HEC- nano SiO_2, 2-HEC- *(hf)* nano SiO_2 XRD spectrum), the angle of 2Θ: 12°, where the maximum peak intensity of cellulose is given in the literature, was observed at 21° in the cross-linked film (Taghizadeh & Seifi-Aghjekohal, 2015). The polycrystalline peaks between 25 and 50° belong to the structure of ceric ammonium nitrate (CAN) (Moorthy & Pitchumani, 2009). The angles of 2Θ; 29.2, 31.4, 34.7, 41.6, and 48.6° correspond to the planes of the tetragonal crystal structure of CAN (Itshak-Levy et al., 2020). In addition, the crystal structure of the CAN-supported cellulose derivatives is preserved, which can be seen in Figs. 5 and 6 (Dhakshinamoorthy & Pitchumani, 2009).

In the XRD spectrum in Fig. 6, the effect of amine modified SiO_2 on HPMC nanocomposite films is given. According to the results, even if the intensity drops, the surface crystallinity of cellulose structures was improved by adding nano SiO_2. In the literature, HPC peaks give wide peaks between 6 and 8° and 15–20° (Wang et al., 2006). According to the XRD pattern results of cross-linked HPC, HPC - nano SiO_2, and HPC – *(hf)* nano SiO_2 (Fig. 6 (continued)), the cross-linked HPC films shift to slightly higher degrees (7° and 19°). After nano SiO_2 doping, the broad peaks narrowed, and the intensity increased. It can be explained that cross-linking also plays a role in the change of peak intensities.

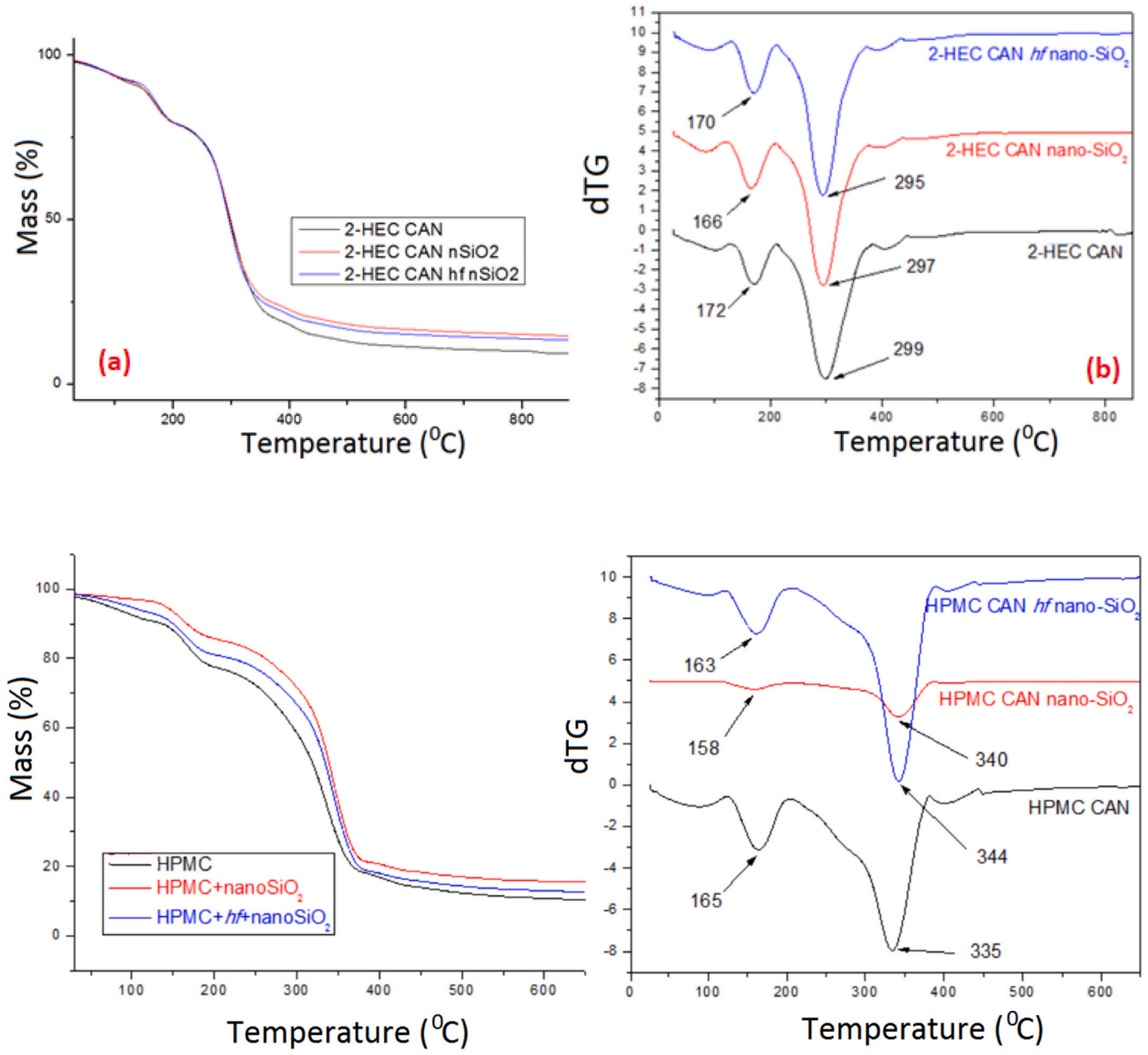

Fig. 8. TGA and DTG curves of doped and plain cross-linked 2-HEC films.

4.3. SEM analysis

Nano SiO_2 and cross-linking changes of the film surfaces were observed with SEM images. The morphological images of hydrophilic amine-modified nano SiO_2 doped, neutral nano SiO_2 doped and plain 2-HEC, HPC, and HPMC cellulose films are given in Fig. 7. SEM images were taken at the same magnification for each film (5000 x). It is seen that particles agglomerate in their partial places with the doping of nano SiO_2 on the plain 2-HEC film. In previous studies, the hydrophilic and/or hydrophobic nature of nanoparticles doped on 2-HEC films had a similar effect (Azzaoui et al., 2015). The denser structure of 5 % solution of HPMC than other celluloses increased the surface roughness in nano SiO_2 doped composite films compared to plain ones. The amine modified hydrophilic nano SiO_2 is highly homogeneously compatible with the HPC structure. Nano SiO_2 amounts in cellulose films were optimized. The best compatibility between matrix and reinforcements was selected for the test and analysis, in this study. Different amounts of nano SiO_2 effect on cellulose films' (with and without cross-linking agent) surface was given in Figs. S1. and S2. SEM images of cross-linked 2-HEC films showing increasing nano SiO_2 distributions are given in Fig. S2. It was observed that the surface smoothness of the crosslinked films increased with the crosslinker compared to the non-crosslinked films.

4.4. TGA analysis

The thermal behaviors of the 2-HEC films produced are given in Fig. 8. High intense endothermic peaks were observed in DTA curves between 150 and 350 °C. At this temperature range, an overall mass loss was found for the nano SiO_2 doped and plain 2-HEC films compared to the TG curves. As the temperature increased, the slope of the TG curves of the films changed horizontally. These mass losses are explained by the depolymerization of cellulose ether (Angelova et al., 2019). In the literature, the degradation of 2-HEC is given between 300 and 350 °C (Yang et al., 2016). In the degradation curves given in Fig. 8, it has seen

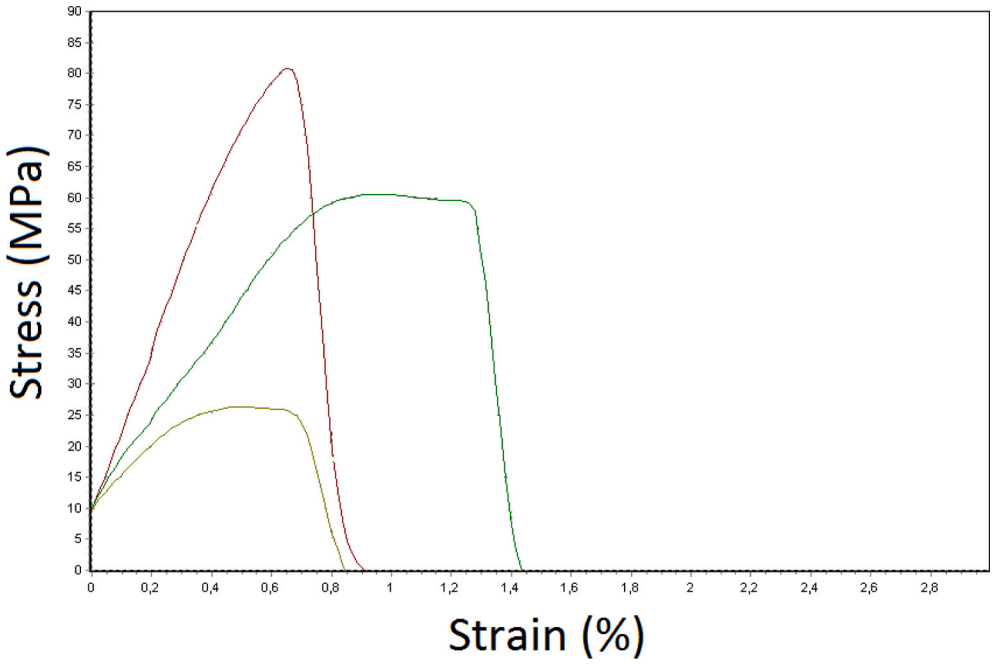

Fig. 9. Stress-strain curves of crosslinked HPMC (red line), nano SiO_2 doped HPMC (brown line) and amine modified hydrophilic nano SiO_2 doped HPMC (green line) nanocomposites. (For interpretation of the references to colour in this figure legend, the reader is referred to the web version of this article.)

Table 1
Mechanical test results of cross-linked cellulosic nanocomposite films.

	Stress, σ (MPa)	Strain, ε (%)
2-HEC CAN	29,3	106
2-HEC CAN nano SiO_2	17,4	105,7
2-HEC CAN *hf* nano SiO_2	30,6	106,2
HPMC CAN	72,6	101,4
HPMC CAN nano SiO_2	37	100,85
HPMC CAN *hf* nano SiO_2	71,6	101,7

that CAN decomposes in the first step and silica reinforced 2-HEC films decompose in the second step. When the DTG curves were examined, the maximum decomposition temperature of the plain film decreased by 2–4 °C by doping nano SiO_2 and amine-modified nano SiO_2 to 2-HEC films. DTG curves of 2-HEC and cross-linked 2-HEC films for comparison effect of CAN were given in Fig. S3. Also, the mechanism of cross-linking between Ce^{4+} ions and cellulose was given in Fig. S4.

Thermogravimetric analysis (TGA) showed the temperatures of the degradation steps of cellulose because of its crosslinking (Sotolarova et al., 2021). In Fig. 8 (continued), TG and DTG curves of HPMC nanocomposite films are given. In the first step, CAN is separated from the film structure at around 165 °C. The decomposition temperature of HPMC is 335 °C. It was observed that the thermal resistance of nano SiO_2 and amine modified nano SiO_2 doped films increased. In the literature study, the thermal characteristics of HPMC were examined and it was said that the structure deteriorated at 200 °C (Lim et al., 2009). The behavior in cross-linked films is that the structure of the cellulose is strengthened.

4.5. Mechanical test results

The stress-strain test was applied for nanocomposite films. Due to the difficulties encountered during the preparation of HPC nanocomposite films, HPC results are not reflected in the table. In Fig. 9, stress-strain curves of cross-linked HPMC and nano-SiO_2 doped HPMC composite films are given as an example. The red colored curve belongs to the cross-linked HPMC film. As seen in the figure, its resistance to the applied force is quite high, but the amount of strain is low. After nano SiO_2 doping, a decrease was observed in the readings of the stress-strain curves of the cross-linked HPMC film. Considering all previous experimental evaluations, it can be said that this result is normal. Because the surface roughness of nanocomposite films doped with nano SiO_2 increased, deterioration in the integrity of the surface was observed. On the other hand, although the tensile strength is low in amine modified hydrophilic nano-SiO_2 doped nanocomposite films, there has been a significant increase in the amount of strain value since the additive integrates homogeneously with the nanocomposites and provides elasticity to the structure. As a result, we can say that amine modified hydrophilic nano SiO_2 doped composite films will have better performance in target applications.

The results obtained from the stress-strain values of cross-linked 2-HEC and HPMC films are given in Table 1. Test results were calculated by using Eqs. (1) and (2). As can be seen, although the tensile strength is high in HPMC, the strain amount is lower, when compared to 2-HEC. It is possible to say that the strain amount is less than 2-HEC due to the denser chemical arrangement of the HPMC structure.

5. Conclusions

At the end of the study, we confirmed our original hypothesis. The results caused structural, surface, thermal and mechanical changes in cellulose derivatives of silica nanoparticles. In different application areas, silica-added cellulose derivatives with desired properties can be used preferentially. Film formation was observed in all three different cellulose derivatives. Mechanical strength tests were performed as stress-strain measurements on cellulosic films and according to these results, the strength of inorganic added films was found to be increased compared to undoped films. 2-HEC gave the best nanocomposite hydrogel film formation among natural polymers. HPMC did not provide adequate compatibility in terms of viscosity and HPC in terms of difficulty in forming crosslinked films. Cross-linked nanocomposite films obtained with 2-HEC will be the application systems that will be focused on in future studies on the durability of the film. While cellulosic natural polymers/nano SiO_2 dissolve in water when they are not cross-linked, they provide dimensional stability at different times depending on the

difference in the amount of nano SiO_2 in the cross-linked films. In a conclusion, the results of the analysis proved that the dispersion of the reinforcement materials in the cellulose matrix was carried out successfully. In future studies, the biological activities of these nanocomposite films will be examined and tested as artificial human skin in biotechnological application areas.

Declaration of competing interest

The authors declare that they have no known competing financial interests or personal relationships that could have appeared to influence the work reported in this paper.

Data availability

No data was used for the research described in the article.

Acknowledgments

This study includes a part of author Fatma Özge Gökmen's doctoral thesis.

References

Akinosho, H., Hawkins, S., & Wicker, L. (2013). Hydroxypropyl methylcellulose substituent analysis and rheological properties. *Carbohydrate Polymers, 98*, 276–281.

Angelova, T., Rangelova, N., Georgieva, N., Nemska, V., Stoyanova, T., Uzunova, V., Aleksandrov, L., & Tzoneva, R. (2019). Study of potential biomedical application of sol-gel derived zn-doped SiO2- hydroxypropyl cellulose nanohybrids. *Materials Science & Engineering C, 100*, 608–615.

Angelova, T., Rangelova, N., Yurgev, R., Georgieva, N., & Müller, R. (2012). Antibacterial activity of SiO2 / hydroxy propyl cellulose hybrid materials containing silver nanoparticles. *Materials Science and Engineering C, 32*, 1241–1246.

Antosik, A. K., Piątek, A., & Wilpiszewska, K. (2019). Carboxymethylated starch and cellulose derivatives-based film as human skin equivalent for adhesive properties testing. *Carbohydrate Polymers, 222*, Article 115014. https://doi.org/10.1016/j.carbpol.2019.115014

Arca, H., Mosquera-Giraldo, L., Bi, V., Xu, D., Taylor, L., & Edgar, K. (2018). Pharmaceutical applications of cellulose ethers and cellulose ether esters. *Biomacromolecules, 19*. https://doi.org/10.1021/acs.biomac.8b00517

Azzaoui, K., Mejdoubi, E., Lamhamdi, A., Zaoui, S., Berrabah, M., Elidrissi, A., Hammouti, B., Fouda, M. M. G., & Al-Deyab, S. S. (2015). Structure and properties of hydroxyapatite/hydroxyethyl cellulose acetate composite films. *Carbohydrate Polymers, 115*, 170–176.

Badulescu, R., Vivod, V., Jausovec, D., & Voncina, B. (2008). Grafting of ethylcellulose microcapsules onto cotton fibers. *Carbohydrate Polymers, 71*(1), 85–91. https://doi.org/10.1016/j.carbpol.2007.05.028

Bao, X., Wang, C., Zhang, Z., Cao, Q., Liu, F., Chen, J., Zhang, C., Na, H., & Zhu, J. (2021). Wet spinning to prepare filaments from three cellulose carbonated derivatives: Synthesis, characterization and filament properties. *Carbohydrate Polymer Technologies and Applications, 2*, Article 100099.

Bettini, S., Pagano, R., Bosco, G., Pal, S., Ingrosso, C., Valli, L., & Giancane, G. (2022). SiO2 based nanocomposite for simultaneous magnetic removal and discrimination of small pollutants in water. *Colloids and Surfaces A: Physicochemical and Engineering Aspects, 633*, Article 127905.

Bettini, S., Santino, A., Valli, L., & Giancane, G. (2015). A smart method for the fast and low-cost removal of biogenic amines from beverages by means of iron oxide nanoparticles. *RSC Advances, 5*, 18167–18171. https://doi.org/10.1039/c5ra01699a

Lu, Y., & Ozcan, S. (2015). Green nanomaterials: On track for a sustainable future. *Nano Today, 10*, 417–420.

Borlinghaus, N., Wittmann, V., & Braje, W. M. (2022). Using polymeric hydroxypropyl methylcellulose as an alternative to 'micellar catalysis' to enable chemical reactions in water. *Current Opinion in Green and Sustainable Chemistry, 33*, Article 100571.

Bulut, E., & Turhan, Y. (2021). Synthesis and characterization of temperature-sensitive microspheres based on acrylamide grafted hydroxypropyl cellulose and chitosan for the controlled release of amoxicillin trihydrate. *International Journal of Biological Macromolecules, 191*, 1191–1203.

Cao, Y., & Tan, H. (2002). Effects of cellulase on the modification of cellulose. *Carbohydrate Research, 337*(14), 1291–1296. https://doi.org/10.1016/S0008-6215(02)00134-9

Chen, W., Yu, H., Lee, S. Y., Wei, T., Li, J., & Fan, Z. (2018). Nanocellulose: A promising nanomaterial for advanced electrochemical energy storage. *Chemical Society Reviews, 47*, 2837–2872.

Cristea, M. V., Riedl, B., & Blanchet, P. (2010). Enhancing the performance of exterior waterborne coatings for wood by inorganic nanosized UV absorbers. *Progress in Organic Coating, 69*, 432–441. https://doi.org/10.1016/j.porgcoat.2010.08.006

Dhakshinamoorthy, A., & Pitchumani, K. (2009). Clay-supported ceric ammonium nitrate as an effective, viable catalyst in the oxidation of olefins, chalcones and sulfides by molecular oxygen. *Catalysis Communications, 10*, 872–878. https://doi.org/10.1016/j.catcom.2008.12.025

Du, H., Liu, C., Zhang, M., Kong, Q., Li, B., & Xian, M. (2018). Preparation and industrialization status of nanocellulose. *Progress in Chemistry, 30*(4), 448. https://doi.org/10.7536/PC170830

Du, H., Parit, M., Wu, M., Che, X., Wang, Y., Zhang, M., et al. (2020). Sustainable valorization of paper mill sludge into cellulose nanofibrils and cellulose nanopaper. *Journal of Hazardous Materials, 400*(5), Article 123106. https://doi.org/10.1016/j.jhazmat.2020.123106

Esmaeilirad, N., White, S., Terry, C., Prior, A., & Carlson, K. (2016). Influence of inorganic ions in recycled produced water on gel-based hydraulic fracturing fluid viscosity. *Journal of Petroleum Science and Engineering, 139*, 104–111. https://doi.org/10.1016/j.petrol.2015.12.021

Fathi, M., Sodeifian, G., & Sajadian, S. A. (2022). Experimental study of ketoconazole impregnation into polyvinyl pyrrolidone and hydroxyl propyl methyl cellulose using supercritical carbon dioxide: Process optimization. *The Journal of Supercritical Fluids, 188*, Article 105674. https://doi.org/10.1016/j.supflu.2022.105674

Filippo, M. F. D., Dolci, L. S., Liccardo, L., Bigi, A., Bonvicini, F., Gentilomi, G. A., Passerini, N., Panzavolta, S., & Albertini, B. (2021). Cellulose derivatives-snail slime films: New disposable eco-friendly materials for food packaging. *Food Hydrocolloids, 111*, Article 106247. https://doi.org/10.1016/j.foodhyd.2020.106247

Fufa, S. M., Jelle, B. P., Hovde, P. J., Jelle, P. B., & Hovde, J. P. (2013). Weathering performance of spruce coated with water based acrylic paint modified with TiO2 and clay nanoparticles. *Progress in Organic Coating, 76*, 1543–1548. https://doi.org/10.1016/j.porgcoat.2013.06.008

Gabriel, M., Santos, O. M., Costa, L. M., Daltro, P., Basmaji, P., et al. (2014). Physically modified bacterial cellulose biocomposites for guided tissue regeneration. *Science of Advanced Materials, 6*, 2673–2678. https://doi.org/10.1166/sam.2014.1985

Gopi, S., Balakrishnan, P., Chandradhara, D., Poovathankandy, D., & Thomas, S. (2019). General scenarios of cellulose and its use in the biomedical field. *Materials Today Chemistry, 13*, 59–78.

Hoang, P. H., & Dat, N. M. (2021). Study on using cellulose derivatives as pore directing agent for preparation of hierarchical ZSM-5 zeolite catalyst. *Advanced Powder Technology, 32*, 3927–3933.

Hu, J., Liu, Y., Zhang, M., He, J., & Ni, P. (2020). A separator based on cross-linked nano-SiO2 and cellulose acetate for lithium-ion batteries. *Electrochimica Acta, 334*, Article 135585.

Itshak-Levy, D., Israel, L. L., Schmerling, B., Kannan, S., Sade, H., Michaeli, S., & Lellouche, J. P. (2020). Disaggregation, stabilization, and innovative functionalization/surface engineering of detonation nanodiamonds via ultrasonication-promoted ceric ammonium nitrate treatment. *Diamond & Related Materials, 104*, Article 107738. https://doi.org/10.1016/j.diamond.2020.107738

Jedvert, K., & Heinze, T. (2017). Cellulose modification and shaping-a review. *Journal of Polymer Engineering, 37*(9), 845–860. https://doi.org/10.1515/polyeng-2016-0272

Josmin, P. J., & Kuruvilla, J. (2012). Advances in polymer composites: Macro-and microcomposites—State of the art, new challenges, and opportunities. In S. Thomas, J. Kuruvilla, S. Malhotra, K. Goda, & M. S. Sreekala (Eds.), *Polymer composites* (pp. 3–16). Weinheim: Wiley.

Kargarzadeh, H., Mariano, M., Gopakumar, D., Ahmad, I., Thomas, S., Dufresne, A., et al. (2018). Advances in cellulose nanomaterials. *Cellulose, 25*(4), 2151–2189. https://doi.org/10.1007/s10570-018-1723-5

Liu, W., Du, H., Liu, H., Xie, H., Xu, T., Zhang, X., et al. (2020). Highly efficient and sustainable preparation of carboxylic and thermostable cellulose nanocrystals via FeCl3-catalyzed innocuous citric acid hydrolysis. *ACS Sustainable Chemistry & Engineering, 8*(44), 16691–16700. https://doi.org/10.1021/acssuschemeng.0c06561

Kesevan, S. K., Selvaraj, D., Perumal, S., Arunachalakasi, A., Ganesan, N., Chinnaiyan, S. K., & Balaraman, M. (2022). Fabrication of hybrid povidone-iodine impregnated collagen-hydroxypropyl methylcellulose composite scaffolds for wound-healing application. *Journal of Drug Delivery Science and Technology*. , Article 103247. https://doi.org/10.1016/j.jddst.2022.103247

Kulshrestha, A. S., & Mahapatro, A. (2008). Polymers for biomedical applications. *ACS Symposium Series, 977*, 1–7.

Li, X., Zhang, K., Shi, R., Ma, X., Tan, L., Ji, Q., et al. (2017). Enhanced flame-retardant properties of cellulose fibers by incorporation of acid-resistant magnesium-oxide microcapsules. *Carbohydrate Polymers, 176*, 246–256. https://doi.org/10.1016/j.carbpol.2017.08.096

Lim, W. S., Choi, J. W., Iwata, Y., & Koseki, H. (2009). Thermal characteristics of hydroxypropyl methyl cellulose. *Journal of Loss Prevention in the Process Industries, 22*, 182–186.

Liu, K., Du, H., Zheng, T., Liu, H., Zhang, M., Zhang, R., Li, H., Xie, H., Zhang, X., Ma, M., & Si, C. (2021). Recent advances in cellulose and its derivatives for oilfield applications. *Carbohydrate Polymers, 259*, Article 117740.

Luo, C., Huang, Y., Yin, Z., Xu, H., Qin, X., Li, X., Wang, M., & Lin, Y. (2020). A universal natural hydroxy propyl methyl cellulose polymer additive for modifying lignocellulose-based gel polymer electrolytes and stabilizing lithium metal anodes. *Materials Chemistry and Physics, 250*, Article 123174.

Marinho, F. M. (2013). In *Cellulose and its derivatives use in the pharmaceutical compounding practice* (pp. 141–162).

Menon, M. P., Selvakumar, R., Kumar, P. S., & Ramakrishna, S. (2017). Extraction and modification of cellulose nanofibers derived from biomass for environmental application. *RSC Advances, 7*(68), 42750–42773. https://doi.org/10.1039/C7RA06713E

Moon, R. J., Martini, A., Nairn, J., Simonsen, J., & Youngblood, J. (2011). Cellulose nanomaterials review: Structure, properties and nanocomposites. *Chemical Society Reviews, 40*(7), 3941–3994. https://doi.org/10.1039/C0CS00108B

Moorthy, A. D., & Pitchumani, K. (2009). Clay supported ceric ammonium nitrate as an effective, vilable catalyst in the oxidation of olefins, chalcones and sulfides by molecular oxygen. *Catalysis Communications, 10*, 872–878.

Mutalik, V., Manjeshwar, L. S., Wali, A., Sairam, M., Raju, K. V. S. N., & Aminabhavi, T. M. (2006). Thermodynamics/hydrodynamics of aqueous polymer solutions and dynamic mechanical characterization of solid films of chitosan, sodium alginate, guar gum, hydroxy ethyl cellulose and hydroxypropyl methylcellulose at different temperatures. *Carbohydrate Polymers, 65*, 9–21.

Nasir, M., Subhan, A., Prihandoko, B., & Lestariningsih, T. (2017). Nanostructure and property of electrospun SiO2-cellulose acetate nanofiber composite by electrospinning. *Energy Procedia, 107*, 227–231.

Pacheco, C. M., Cecilia, B. A., Reyes, G., Oviedo, C., Fernandez-Perez, A., Elso, M., & Rojas, O. J. (2021). Nanocomposite additive of SiO2/TiO2/nanocellulose on waterborne coating formulations for mechanical and aesthetic properties stability on wood. *Materials Today Communications, 29*, Article 102990.

Petit, J. Y., & Wirquin, E. (2013). Evaluation of various cellulose ethers performance in ceramic tile adhesive mortars. *International Journal of Adhesion and Adhesives, 40*, 202–209. https://doi.org/10.1016/j.ijadhadh.2012.09.007

Ramakrishna, S., Mayer, J., Wintermantel, E., & Leong, K. W. (2001). Biomedical applications of polymer-composite materials: A review. *Composites Science and Technology, 61*(9), 1189–1224.

Rangelova, N., Aleksandrov, L., & Nenkova, S. (2018). Synthesis and characterization of pectin/SiO2 hybrid materials. *Journal of Sol-Gel Science and Technology, 85*(2), 330–339.

Regan, J., Dolores, J., Lepore, M., Gualano, M., Badson, J., Zimnoch, A., Capitani, J. F., & Fan, J. (2019). Modified silica gels as recyclable adsorbents of aqueous polycyclic aromatic hydrocarbons. *Green Chemistry Letters and Reviews, 12*, 435–443. https://doi.org/10.1080/17518253.2019.1687760

Roshan, H., & Asef, M. R. (2010). Characteristics of oilwell cement slurry using CMC. *SPE Drilling & Completion, 25*(03), 328–335. https://doi.org/10.2118/114246-PA

Saraiva, S., Pereira, P., Paula, C. T., Rebelo, R. C., Coelho, J. F. J., Serra, A. C., & Fonseca, A. C. (2021). Development of electrospun mats based on hydrophobic hydroxypropyl cellulose derivatives. *Materials Science & Engineering C, 131*, Article 112498.

Sayyed, A. J., Deshmukh, N. A., & Pinjari, D. V. (2019). A critical review of manufacturing processes used in regenerated cellulosic fibres: Viscose, cellulose acetate, cuprammonium, LiCl/DMAc, ionic liquids, and NMMO based lyocell. *Cellulose, 26*(5), 2913–2940. https://doi.org/10.1007/s10570-019-02318-y (London, England)

Song, R., Murphy, M., Li, C., Ting, K., Soo, C., & Zheng, Z. (2018). Current development of biodegradable polymeric materials for biomedical applications. *Drug Design Development and Therapy, 12*, 3117.

Sotolarova, J., Vinter, S., & Filip, J. (2021). Cellulose derivatives crosslinked by citric acid on electrode surface as a heavy metal absorption/sensing matrix. *Colloids and Surfaces A: Physicochemical and Engineering Aspects, 628*, Article 127242.

Sow, C., Riedl, B., & Blanchet, P. (2011). UV-waterborne polyurethane-acrylate nanocomposite coatings containing alumina and silica nanoparticles for wood: Mechanical, optical, and thermal properties assessment. *Journal of Coating Technology and Research, 8*, 211–221. https://doi.org/10.1007/s11998-010-9298-6

Spirk, S. (2018). Polysaccharides in batteries. In S. Spirk (Ed.), *Polysaccharides as battery components* (pp. 9–57). Springer International Publishing. https://doi.org/10.1007/978-3-319-65969-5_2.

Taghizadeh, M. T., & Seifi-Aghjekohal, P. (2015). Sonocatalytic degradation of 2-hydroxyethyl cellulose in the presence of some nanoparticles. *Ultrasonics Sonochemistry, 26*, 265–272.

Tu, H., Zhu, M., Duan, B., & Zhang, L. (2020). Recent progress in high-strength and robust regenerated cellulose materials. *Advanced Materials*. , Article 2000682. https://doi.org/10.1002/adma.202000682

Udayakantha, M., Cho, J., Lu, K. W., Mukhopadhyay, A., Gupta, S., & Hong, C. (2019). An evaluation of the reduction of heat loss enabled by halloysite modification of oilwell cement. *Engineering Research Express*, 1. https://doi.org/10.1088/2631-8695/ab5207

Wang, C., Tan, H., Dong, Y., & Shao, Z. (2006). Trimethylsily hydroxypropyl cellulose: Preparation, properties and as precursors to graft copolymerization of ε-caprolactone. *Reactive & Functional Polymers, 66*, 1165–1173.

Wang, H., Xie, H., Du, H., Wang, X., Liu, W., Duan, Y., et al. (2020). Highly efficient preparation of functional and thermostable cellulose nanocrystals via H2SO4 intensified acetic acid hydrolysis. *Carbohydrate Polymers, 239*, Article 116233. https://doi.org/10.1016/j.carbpol.2020.116233

Wang, S., Lu, A., & Zhang, L. (2016). Recent advances in regenerated cellulose materials. *Progress in Polymer Science, 53*, 169–206.

Wang, Y., Wang, J., Sun, Q., Xu, X., Li, M., & Xie, F. (2022). Hydroxypropyl methylcellulose hydrocolloid systems: Effect of hydroxypropy group content on the phase structure, rheological properties and film characteristics. *Food Chemistry, 379*, Article 132075.

Wohlert, M., Benselfelt, T., Wågberg, L., et al. (2022). Cellulose and the role of hydrogen bonds: Not in charge of everything. *Cellulose, 29*, 1–23. https://doi.org/10.1007/s10570-021-04325-4

Yamane, C., Hirase, R., Miyamoto, H., Kuwamoto, S., & Yuguchi, Y. (2015). Mechanism of structure formation and dissolution of regenerated cellulose from cellulose/aqueous sodium hydroxide solution and formation of molecular sheets deduced from the mechanism. *Cellulose, 22*(5), 2971–2982. https://doi.org/10.1007/s10570-015-0714-z (London, England)

Yang, P., Li, T. B., Wu, M. H., Zhu, X. W., & Sun, X. Q. (2015). Analysis of the effect of polyanionic cellulose on viscosity and filtrate volume in drilling fluid. *Materials Research Innovations, 19*, 5–12. https://doi.org/10.1179/1432891715Z.0000000001329

Yang, Y., Guo, Y., Sun, R., & Wang, X. (2016). Self-assembly and β-carotene loading capacity of hydroxyethyl cellulose—graft-lioleic acid nanomicelles. *Carbohydrate Polymers, 145*, 56–63.

Yuan, Z., Zhang, J., Jiang, A., Lv, W., Wang, Y., Geng, H., et al. (2015). Fabrication of cellulose self-assemblies and high-strength ordered cellulose films. *Carbohydrate Polymers, 117*, 414–421. https://doi.org/10.1016/j.carbpol.2014.10.003

Zhang, C., Yang, X., Li, Y., Qiao, C., Wang, S., Wang, X., Xu, C., Yang, H., & Li, T. (2020). Enhancement of a zwitterionic chitosan derivative on mechanical properties and antibacterial activity of carboxymethyl cellulose-based films. *International Journal of Biological Macromolecules, 159*, 1197–1205. https://doi.org/10.1016/j.ijbiomac.2020.05.080